The florid plaques, which are the pathological hallmark of vCJD, are also found in atypical dCJD cases, although they are more abundant in number in vCJD than atypical dCJD cases. These florid plaques distribute widely in the cerebrum and cerebellum but are only occasionally seen in the thalamus in both CJD cases. However, the pathological features of the thalamus are different between these CJD cases. In atypical dCJD cases, spongiform change, neuronal loss and astrocytosis were reported to be intense especially in anterior and medial nuclei.[5] In vCJD cases, while spongiform change is focally seen in anterior and medial thalamic nuclei and pulvinar nuclei are relatively spared from spongiform change, there is extensive neuronal loss with marked astrocytosis in the pulvinar nuclei.[17] In our case, the neuronal loss and astrocytosis were markedly noted in pulvinar nucleus rather than anterior and medial nuclei. Thus, because the pulvinar nucleus of our case presented marked neuronal loss and astrocytosis as well as severe spongiform change and numerous florid plaques, the pathological features of our case was considered to be distinct from those of reported atypical dCJD and vCJD cases.

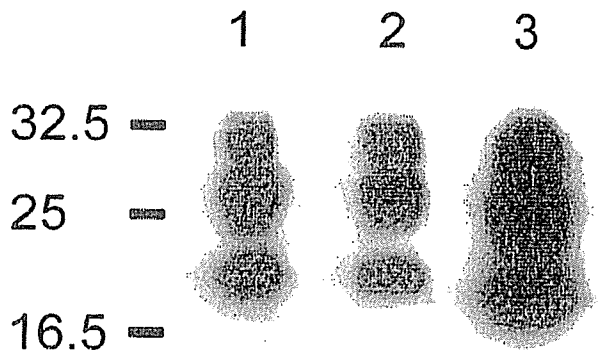

Fig. 3 Immunoblotting. Lane 1, positive control showing type 1 PrP glycoform pattern; lane 2, present study; lane 3, positive control showing type 2 PrP glycoform pattern. The abnormal PrP molecules in the brain homogenates of this case (lane 2) exhibit a type 1 PrP glycoform pattern. Molecular sizes (kDa) are indicated on the left.

Pulvinar increased signals greater than all other basal ganglia on T2-weighted, proton density-weighted, and diffusion-weighted MRI found in our case were unique features and have not been observed in other atypical dCJD cases. The hyperintensity of these images is thought to correlate with the astrocytosis and neuronal loss observed in histological examination.[9] On the other hand, the Gd-DTPA enhancement of the pulvinar nuclei has not been reported in any type of CJD cases. Because the left frontal lesion of the contusion as well as the pulvinar nuclei were enhanced with Gd-DTPA, and because the increased pulvinar signals were asymmetrical and more intense on the left side, these hyperintense signals might reflect damage of the pulvinar nuclei due to a contusion in the left basal forebrain. However, although the thalamus has direct reciprocal connection to the cerebral cortices, the pulvinar nucleus make connections not with the frontal lobe but with the occipital cortex including the striate cortex.[18] In addition, the common pathological findings of the Gd-DTPA-enhancing lesions, the left pulvinar nucleus and the rim of the contusion in the left basal forebrain, was severe astrogliosis. While Gd-DTPA enhancement indicates vascular leakage in general, Gd-DTPA enhancement associated with astrogliosis has also been reported.[19] Therefore, although the precise reason was not clear, we considered that the increased pulvinar signals of our case would reflect pathological changes including severe astrogliosis caused not by traumatic brain injury but by CJD.

The marked pulvinar hyperintensity compared with all other basal ganglia recognized in our case raised the concern of vCJD because the asymmetrical pulvinar hyperintensity has previously been detected in some neuropathologically confirmed vCJD cases.[20] However, the radiological hallmark of vCJD, the pulvinar sign, is defined as symmetrical hyperintensity. Thus, the lack of symmetry in our case was not identical to the radiological features of vCJD cases. In addition, the proposed diagnostic criteria excluded the classification of our case as vCJD after possible iatrogenic exposure.[16] Moreover, the PrP glycoform pattern of our case was type 1 according to Parchi's classification, and was identical to those of reported atypical dCJD cases but was completely different from that of vCJD.[1]

Fig. 2 Verification of abnormal PrP deposition by histological examination. (A–C) HE staining. (D–I) Immunohistochemistry probed with an anti-prion protein antibody (monoclonal, clone 3F4, Senetek, Maryland Heights, MO, USA). Severe spongiform change, neuronal loss, and astrocytosis occurred in the left middle frontal lobe (A) and left pulvinar nucleus of the thalamus (B). (C) A prion protein plaque is surrounded by spongiform changes, to give the appearance of a florid plaque in the pulvinar nucleus. There are many prion plaques in the left middle frontal lobe (D) and in the left pulvinar nucleus of the thalamus (E). (F) The core of the florid plaque is intensely immunostained. (G) Unique prion protein depositions are linearly aligned with the neuronal axon in the left cingulate gyrus. (H) Prion protein deposition occurred around the neuronal cell body and process in the left cingulate gyrus. (I) Granular prion protein deposits are present around the wall of a blood vessel in the left pulvinar nucleus of the thalamus. Bars (A,B,D,E,H) 30 μm, (C,F) 15 μm, (G,I) 60 μm.

Therefore, we concluded our case to be atypical dCJD with radiological and pathological characteristics distinct from those of any dCJD cases.

ACKNOWLEDGMENTS

We thank Ms. K. Hatanaka for her excellent technical assitance.

REFERENCES

1. Satoh K, Muramoto T, Tanaka T *et al.* Association of an 11–12 kDa protease-resistant prion protein fragment with subtypes of dura graft-associated Creutzfeldt-Jakob disease and other prion diseases. *J Gen Virol* 2003; **84**: 2885–2893.
2. Kimura K, Nonaka A, Tashiro H *et al.* Atypical form of dural graft associated Creutzfeldt-Jakob disease: report of a postmortem case with review of the literature. *J Neurol Neurosurg Psychiatry* 2001; **70**: 696–699.
3. Kopp N, Streichenberger N, Deslys JP, Laplanche JL, Chazot G. Creutzfeldt-Jakob disease in a 52-year-old woman with florid plaques. *Lancet* 1996; **348**: 1239–1240.
4. Kretzschmar HA, Sethi S, Földvári Z *et al.* Iatrogenic Creutzfeldt-Jakob disease with florid plaques. *Brain Pathol* 2003; **13**: 245–249.
5. Shimizu S, Hoshi K, Muramoto T *et al.* Creutzfeldt-Jakob disease with florid-type plaques after cadaveric dura mater grafting. *Arch Neurol* 1999; **56**: 357–362.
6. Takashima S, Tateishi J, Taguchi Y, Inoue H. Creutzfeldt-Jakob disease with florid plaques after cadaveric dural graft in a Japanese woman. *Lancet* 1997; **350**: 865–866.
7. Lane KL, Brown P, Howell DN *et al.* Creutzfeldt-Jakob disease in a pregnant woman with an implanted dura mater graft. *Neurosurgery* 1994; **34**: 737–740.
8. Mochizuki Y, Mizutani T, Tahiri N *et al.* Creutzfeldt-Jakob disease with florid plaques after cadaveric dura mater graft. *Neuropathology* 2003; **23**: 136–140.
9. Collie DA, Sellar RJ, Zeidler M, Colchester ACF, Knight R, Will RG. MRI of Creutzfeldt-Jakob disease: imaging features and recommended MRI protocol. *Clin Radiol* 2001; **56**: 726–739.
10. Zeidler M, Sellar RJ, Collie DA *et al.* The pulvinar sign on magnetic resonance imaging in variant Creutzfeldt-Jakob disease. *Lancet* 2000; **355**: 1412–1418.
11. Parchi P, Giese A, Capellari S *et al.* Classification of sporadic Creutzfeldt-Jakob disease based on molecular and phenotypic analysis of 300 subjects. *Ann Neurol* 1999; **46**: 224–233.
12. Santos JMG, Corbalán JAL, Martinez-Lage JF, Guillén JS. CT and MRI in iatrogenic and sporadic Creutzfeldt-Jakob disease: as far as imaging perceives. *Neuroradiology* 1996; **38**: 226–231.
13. Schröter A, Zerr I, Henkel K, Tschampa HJ, Finkenstaedt M, Poser S. Magnetic rosonance imaging in the clinical diagnosis of Creutzfeldt-Jakob disease. *Arch Neurol* 2000; **57**: 1751–1757.
14. Yoon SS, Chan S, Chin S, Lee K, Goodman RR. MRI of Creutzfeldt-Jakob disease: asymmetric high signal intensity of the basal ganglia. *Neurology* 1995; **45**: 1932–1933.
15. Brown P, Preece M, Sato T *et al.* Iatrogenic Creutzfeldt-Jakob disease at the millennium. *Neurology* 2000; **55**: 1075–1081.
16. Will RG, Zeidler M, Stewart GE *et al.* Diagnosis of new variant Creutzfeldt-Jakob disease. *Ann Neurol* 2000; **47**: 575–582.
17. Ironside JW, McCardle L, Horsburgh A *et al.* Pathological diagnosis of variant Creutzfeldt-Jakob disease. *APMIS* 2002; **110**: 79–87.
18. Carpenter MB, Sutin J. Diencephalon. In: Carpenter MB, Sutin J (eds). *Human Neuroanatomy*, 8th edn. Baltimore: Williams & Wilkins, 1983; 500–524.
19. Nishimura R, Takahashi M, Morishita S *et al.* MR Gd-DTPA enhancement of radiation brain injury. *Radiat Med* 1992; **10**: 109–116.
20. Collie DA, Summers DM, Sellar RJ *et al.* Diagnosing variant Creutzfeldt-Jakob disease with the pulvinar sign: MR imaging findings in 86 neuropathologically confirmed cases. *Am J Neuroradiol* 2003; **24**: 1560–1569.

Neuropathology 2006; 26, 43–49 doi:10.1111/j.1440-1789.2006.00654.x

Original Article

Brain stem lesions in sporadic Creutzfeldt–Jakob disease: A histopathological and immunohistochemical study

Masayuki Shintaku,[1] Chikao Yutani[2] and Katsumi Doh-ura[3]

[1]Department of Pathology, Osaka Red Cross Hospital, Tennoji, Osaka, [2]Department of Life Science, Faculty of Science, Okayama University of Science, Okayama, and [3]Department of Prion Research, Tohoku University Graduate School of Medicine, Aoba, Sendai, Japan

Lesions of the brain stem in sporadic CJD were histopathologically and immunohistochemically investigated using an anti-PrP antibody on ten consecutive autopsy cases. Three major histopathological changes, spongiform changes, neuronal loss and hypertrophic astrocytosis, were employed as parameters of the alterations. The quadrigeminal plate and pontine nuclei were the most severely and consistently affected structures, and immunoreactivity against PrP was seen in these structures. There existed some discrepancies between the severity of the lesions and the intensity of the immunoreactivity against PrP. The medulla oblongata essentially remained normal on histopathological examination, but the inferior olivary nucleus showed prominent PrP deposition. Although the general view that pathological alterations in the brain stem are relatively mild in sporadic CJD was confirmed in this study, lesions of variable degrees which might influence a patient's clinical course were still observed in many structures in the brain stem.

Key words: brain stem, CJD, histopathology, immunohistochemistry, PrP.

INTRODUCTION

The principal neuropathological features seen in a brain affected by sporadic CJD include spongiform changes of the neuropil, loss of neurons, proliferation of hypertrophic astrocytes and, in a subset of cases, the formation of amyloid plaque.[1,2] These changes are most prominent in the neocortex of the cerebrum and are also found in various degrees in the basal ganglia and thalamus. In many cases, the cerebellar cortex is also severely affected and, especially in the panencephalopathic type, the white matter of the cerebrum exhibits remarkable pathological alterations.[3] On the other hand, it is believed that pathological alterations in the brain stem below the level of the mesencephalon are mild in sporadic CJD, although involvement of the pontine base or inferior olivary nucleus has been occasionally described.[1,3–5] This is in contrast to other human prion diseases, such as kuru,[6,7] and also prion diseases of animals, such as scrapie,[8] and bovine spongiform encephalopathy (BSE),[9] in which the brain stem is consistently and severely affected by similar pathological processes.

There exist few reports which detail brain stem lesions in sporadic CJD.[10] We investigated such lesions by histopathological and immunohistochemical methods using an anti-PrP antibody on consecutive autopsy cases of sporadic CJD.

MATERIALS AND METHODS

From the autopsy files of the departments of pathology of the Osaka Red Cross Hospital and the National Cardiovascular Center, ten consecutive autopsy cases of sporadic (non-familial and non-iatrogenic) CJD were retrieved. No case of the variant CJD[11,12] was investigated. A summary of the clinicopathological findings of these cases is presented in Table 1. Analysis of the *PrP* gene had been only performed for the recently autopsied cases (cases 8–10), and in all of these the gene was the wild type and codon 129 was homozygous for methionine.

In all cases, the brain had been routinely examined after formalin fixation. Representative sections taken from many regions of the cerebrum and cerebellum were

Correspondence: Masayuki Shintaku, MD, Department of Pathology, Osaka Red Cross Hospital, Tennoji, Osaka 543-8555, Japan. Email: masa-s@sings.jp

Received 28 March 2005; revised and accepted 30 June 2005.

Table 1 Clinicopathological findings of the cases studied

Case	Age (years)	Gender	Duration (months)	Brain weight (grams)	Prion typing
1	70	F	20	830	
2	77	F	7	1110	
3	59	M	24	850	
4	75	F	35	900	
5	66	M	45	860	
6	67	M	18	1010	
7	71	M	16	Unknown	
8	71	M	7	1140	MM1
9	61	F	7	900	MM1
10	56	F	16	790	MM1

reviewed, and the neuropathological diagnosis of sporadic CJD was confirmed. Each brain stem had been cut in planes vertical to the long axis in all cases, and tissue sections had been taken from four to six different levels extending from the rostral mesencephalon to the caudal medulla oblongata. Paraffin sections had then been stained with HE, luxol fast blue-periodic acid-Schiff, modified Bielschowsky, and Nissl stains. We evaluated the lesions of the gray matter of the brain stem employing the following three histopathological parameters:[1,2] (i) spongiform changes of the neuropil; (ii) loss of neurons; and (iii) the proliferation of hypertrophic astrocytes. Other specific pathological alterations were also recorded. Because there was a subtle difference in the examined levels of sections between the cases because of the retrospective nature of this study, only easily identifiable, distinct nuclear groups were selected for evaluation. Changes in the white matter of the brain stem were excluded, because they were considered to largely represent secondary alterations caused by lesions in the cerebral or cerebellar cortex.

In eight cases for which preserved paraffin blocks were available, sections were recut and immunohistochemical investigations were performed using a monoclonal antibody against PrP (clone 3F4, DakoCytomation, Glostrup, Denmark; 1:100) and by employing the Envision Plus detection system (DakoCytomation) after pretreatment of the sections by hydrolytic autoclaving in 1.5 mmol hydrochloric acid at 121°C for 10 min.[13] Paraffin sections of the medulla oblongata were available only for cases 7–10.

The severity of individual lesions and the intensity of the immunohistochemical reactions were evaluated using the four-tiers grading system: (–) absent or negative; (±) equivocal or very weakly positive; (+) definitely present or positive; and (++) severe or intensely positive.

RESULTS

For the overall neuropathological features of the cerebral hemispheres and the cerebellum, in all cases the brain showed gross atrophy, and the thinning of the cerebral cortex was marked. The cerebellum also exhibited severe cortical atrophy along with the marked depopulation of granule cells and thinning of the molecular layer. No amyloid plaque was observed in any case. The white matter of the cerebral hemispheres showed diffuse myelin pallor and axonal loss. In addition, peculiar, localized spongiform changes of the subcortical white matter, which is a characteristic of panencephalopathic type CJD,[3] were noted in cases 9 and 10.

On gross examination, the mesencephalon and pons showed diffuse atrophy of mild to moderate degree in every case, and the pontine base had lost its bulge on the ventral surface. On the other hand, the medulla oblongata appeared almost normal on macroscopic observation. A summary of the brain stem lesions is presented in Table 2.

Mesencephalon

The superior and inferior colliculi were the most distinctly and consistently affected sites among the structures present in the mesencephalon. Spongiform changes were seen chiefly in the superficial layers, and neuronal loss and astrocytosis were found diffusely throughout these structures (Fig. 1). The periaqueductal gray matter was also involved, but less distinctly than in the quadrigeminal plate, and neuronal loss was not apparent. In case 1, a few senile plaques were observed in this region. Neurons of the oculomotor nucleus were well preserved, but spongiform changes were noted in cases 9 and 10. Of special interest, multiple large vacuoles were occasionally found in the neuronal perikarya in the oculomotor nucleus of these two cases (Fig. 2). In another case (case 3), similar vacuoles in the perikarya were found in several pigmented neurons of the substantia nigra. Pathological alterations in the red nucleus and reticular formation were mild except for case 9, in which spongiform changes and astrocytosis were noted to a moderate degree. In the substantia nigra, neuronal loss to a mild degree was noted in the zona compacta in most cases. Spongiform changes were clearly observed in four cases, and a few "foamy spheroids" were

Table 2 Summary of the histopathological and immunohistochemical findings of the brain stem

		Case 1				Case 2				Case 3				Case 4				Case 5			
		SC	NL	AS	PrP	SC	NL	AS	SC	NL	AS	PrP	SC	NL	AS	PrP	SC	NL	AS	PrP
Mesencephalon	Superior colliculus	–	+	++	+	NE	NE	NE	–	±	++	–	NE	NE	NE	NE	+	±	+	+
	Inferior colliculus	NE	NE	NE	NE	+	±	+	NE	NE	NE	NE	NE	NE	NE	NE	NE	NE	NE	NE
	Periaqued. gray matter	-	–	+	±	+	–	-	-	-	+	-	NE	NE	NE	NE	±	-	±	+
	Oculomotor nucleus	-		+	-	±	–	-	-	-	-	-	NE	NE	NE	NE	±	-	±	±
	Red nucleus	–	–	+	–	NE	NE	NE	–	–	+	–	±	–	+	–	–	–	±	–
	Reticular formation			+	+	±		±			+		NE	NE	NE	NE			±	±
	Subst. nigra, Z. comp.	–	+	+	–	–	–	–	+	+	+	–	++	+	+	–	++	±	±	±
	Subst. nigra, Z. reticu.	–	+	+	–	–	–	–	+	+	+	–	NE	NE	NE	NE	++	±	±	–
Pons	Locus ceruleus		±	+	+	NE	NE	NE	NE	NE	NE	NE	±	±	±					+
	Raphe nucleus	–	–	–	+	NE	NE	NE	–	–	+	+	±	±	±	–	–	–	–	+
	Reticular formation	–	–	–	+	NE	NE	NE	–	–	–	+	–	–	+	–	–	–	–	+
	Pontine nuclei	–	++	++	+	–	–	–	–	+	++	+	-	++	++	-	++	++	++	±
Medulla oblongata	Nucl. N. hypogloss.	–	±	+	NE	–	–	–	–	–	±	NE	–	–	+	NE	–	–	±	NE
	Nucl. dors. n. trigem.	–	–	–	NE	NE	NE	NE	–	–	±	NE	–	–	+	NE	–	–	±	NE
	Nucl. tr. spin. n. trigem.	-			NE	-	-	-	-	-	±	NE	–	-	+	NE	-	-	±	NE
	Raphe nucleus	–	–	–	NE	NE	NE	NE	–	–	±	NE	–	–	–	NE	–	–	±	NE
	Reticular formation	–	–	±	NE	–	–	–	–	–	±	NE	–	–	+	NE	–	–	±	NE
	Olivary nucleus			+	NE						+	NE		+	+	NE		+	+	NE
	Nucl. fasc. poster.	–	–	±	NE	–	–	–	–	–	–	NE	–	–	+	NE	NE	NE	NE	NE

(continued)

		Case 6			Case 7				Case 8				Case 9				Case 10			
		SC	NL	AS	SC	NL	AS	PrP	SC	NL	AS	PrP	SC	NL	AS	PrP	SC	NL	AS	PrP
Mesencephalon	Superior colliculus	+	+	+	+	+	+	+	+	+	+	+	+	+	+	+		+	+	+
	Inferior colliculus	+	+	+	+	+	+	-	NE	NE	NE	NE	NE	NE	NE	NE	-	+	+	++
	Periaqued. gray matter	–	±	+	+	–	+	+	+	–	+	±	+	±	+	+	–	–	+	+
	Oculomotor nucleus	–	–	–	–	–	–	–	±	–	±	±	+	–	+	±	+	–	–	+
	Red nucleus	-		+	–	–	–	.	±	–	±	±	+	–	+	–	-	–	–	–
	Reticular formation	–	–	+	+	–	+	–	±	–	±	±	+	–	+	±	±	–	±	+
	Subst. nigra, Z. comp.	–	+	–	–	+	±	–	±	+	+	±	–	–	±	+	+	±	±	+
	Subst. nigra, Z. reticu.	–	+	+	–	+	±	.	-	–	+	-	-	-	±	±	+	±	±	+
Pons	Locus ceruleus	–	–	–	–	–	–	–	±	–	±	+	–	–	±	+	–	–	–	+
	Raphe nucleus							+				+	+	±	+	±				+
	Reticular formation	-		-	-	–	-	+	±		±	+	+	-	+	±	-	-	-	+
	Pontine nuclei	–	+	+	–	+	+	±	±	+	+	+	±	±	+	+	+	++	++	+
Medulla oblongata	Nucl. N. hypogloss.												±		±					+
	Nucl. dors. n. trigem.	–	–	–	–	–	–	–	–	–	-	±	-	–	–	–	–	–	–	+
	Nucl. tr. spin. n. trigem.	–	–	–	–	–	–	–	–	–	–	±	+	–	+	–	–	–	–	+
	Raphe nucleus	–	–	–	–	–	–	–	–	–	–	±	±	–	±	–	–	–	–	+
	Reticular formation	–	–	-	–	-	-	-	-	-	±	±	+	-	+	+	-	-	+	+
	Olivary nucleus	–	+	+	–	+	+	+	–	+	+	+	+	+	+	+	–	–	+	++
	Nucl. fasc. poster.										+		+		+					++

AS, astrocytosis; NE, not examined; NL, neuronal loss; PrP, prion protein; SC, spongiform change.

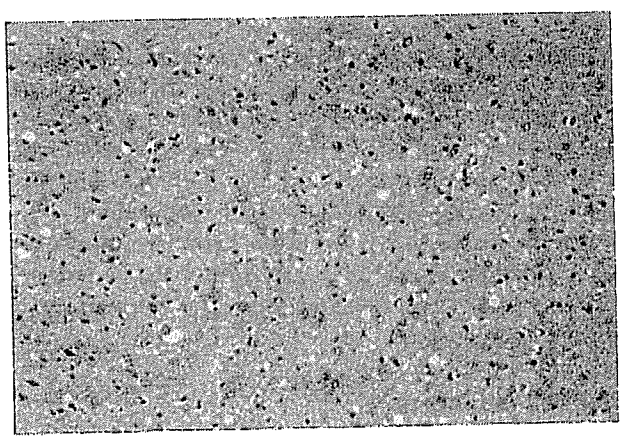

Fig. 1 Spongiform changes of moderate degree associated with neuronal loss and proliferation of hypertrophic astrocytes in the superior colliculus (case 8, HE stain).

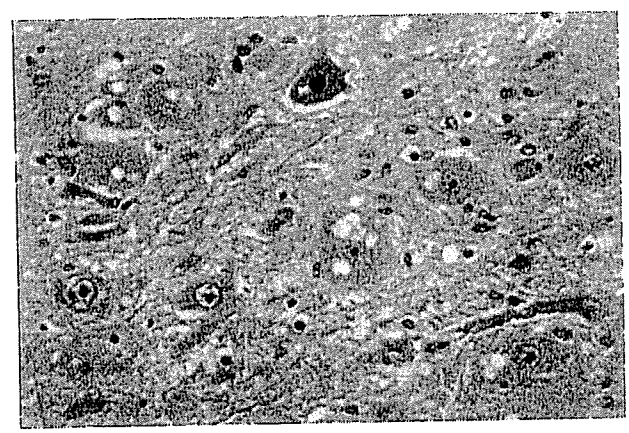

Fig. 2 Multiple large vacuoles found in the neuronal perikarya in the oculomotor nucleus (case 9, HE stain).

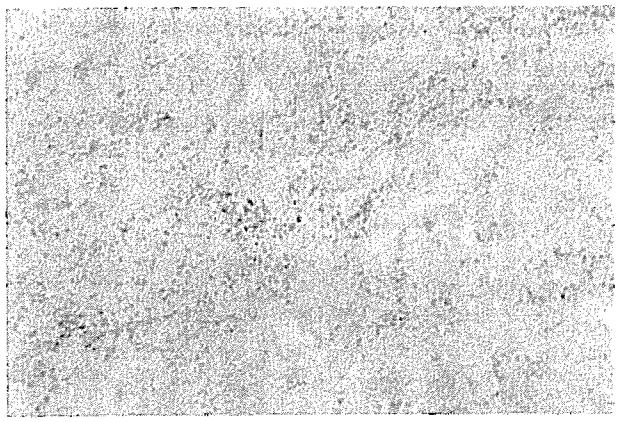

Fig. 3 Diffuse or synaptic type immunoreactivity against PrP in the neuropil of the superior colliculus (case 1, immunostain for PrP).

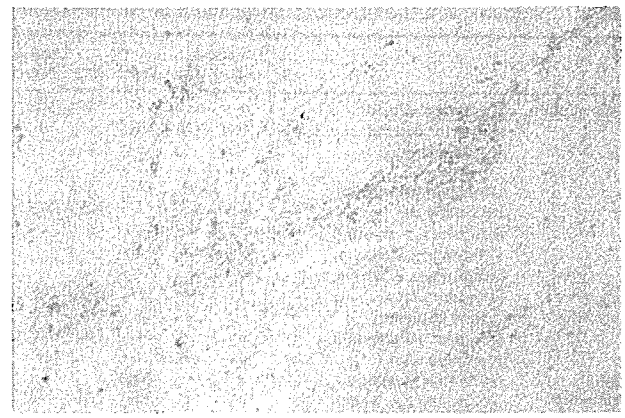

Fig. 5 Prominent deposition of PrP of diffuse or synaptic type in the pontine nuclei (case 8, immunostain for PrP).

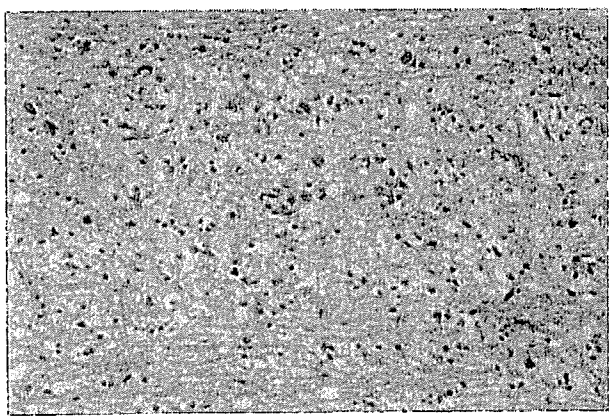

Fig. 4 Severe neuronal loss associated with spongiform changes and astrocytosis in the pontine nuclei. The sizes of the perikarya of the remaining neurons are reduced (case 10, HE stain).

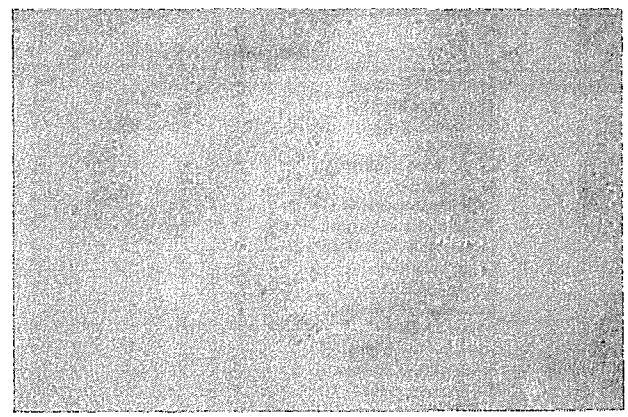

Fig. 6 Neurons of the inferior olivary nucleus were well preserved, but marked deposition of PrP was found in the neuropil (case 10, immunostain for PrP).

occasionally found in the zona reticulata, showing mild astrocytosis.

Diffuse or synaptic-type immunoreactivity against PrP was consistently found in the quadrigeminal plate (Fig. 3), while it was weak or absent in other regions of the mesencephalon, and it roughly paralleled neuronal loss and astrocytosis.

Pons

The histopathological alterations in the pons were almost restricted to the pontine base except for case 9, and the tegmentum was well preserved as a whole. In case 9, spongiform changes accompanied by astrocytosis were seen in the reticular formation and raphe nucleus without apparent neuronal loss. The pontine base was affected in nine of the ten cases, and the loss of neurons of moderate to marked degree in association with hypertrophic astrocytosis was observed in the pontine nuclei (Fig. 4), while spongiform changes in the pontine nuclei were observed only in cases 5 and 10. The sizes of the perikarya of the remaining neurons in the pontine nuclei were reduced as a whole.

Diffuse or synaptic-type immunoreactivity against PrP was noted throughout all gray matter structures in the pons except in case 4, but was most prominent in the pontine nuclei (Fig. 5).

Medulla oblongata

The medulla oblongata was essentially histopathologically normal in all cases. In case 9, only mild spongiform changes accompanied by astrocytosis were noted throughout all

gray matter structures of the medulla oblongata, but no neuronal loss was observed in the tegmentum. The inferior olivary nucleus showed mild neuronal loss and astrocytosis in six cases, but these changes were considered most likely to be an age-related phenomenon and not of pathological nature. Axonal spheroids (dystrophic axon terminals) were consistently found in the gracile nucleus.

The results of anti-PrP immunohistochemistry, which was performed in four cases, were not anticipated based on the histopathological findings. Distinct, diffuse or synaptic-type immunoreactivity was noted throughout the inferior olivary nucleus in every case (Fig. 6). In addition, the tegmental structures showed diffuse immunoreactivity in case 10.

DISCUSSION

In sporadic CJD, the brain stem is comparatively spared from pathological alterations, and this is a characteristic of sporadic CJD,[1,4,5] a condition which is distinct from kuru[6,7] or prion diseases in animals such as scrapie[8] and BSE[9] in which the brain stem is severely affected. A previous western immunoblot analysis of the intracerebral distribution of infectious amyloid protein (PrP) in human spongiform encephalopathy revealed the almost complete absence of amyloid protein in the brain stem in sporadic CJD.[14] On the other hand, in variant CJD spongiform changes are occasionally found in the periaqueductal gray matter and pontine nuclei, and neuronal loss with astrocytosis can be seen in structures such as the superior and inferior colliculi, periaqueductal gray matter, inferior olivary nucleus and dorsal vagal nucleus.[12] It is unknown at present why this difference in the distribution of lesions occurs among various kinds of prion disease. In sporadic CJD, the brain stem is less vulnerable or resistant to lesions caused by PrP. It is therefore intriguing to observe in full detail the pathological alterations of the brain stem in sporadic CJD, because progression of the disease might be slower in the brain stem than in the cerebral or cerebellar cortex. By close observation of the brain stem lesions, we might be able to determine the pathological changes in the early stages of the disease.

The results obtained in the present study supported the general view that the brain stem lesions are of mild degree in sporadic CJD. However, on closer examination, some specific and non-specific lesions of variable degree were found at various sites, and this is a phenomenon which is similar with the lesions seen in the hippocampus in sporadic CJD.[15] We discuss some of the brain stem lesions observed and make brief comments on each topic below.

1 We adopted three histopathological parameters[1,2] to evaluate the brain stem lesions, spongiform changes of the neuropil, neuronal loss and hypertrophic astrocytosis, but they did not necessarily occur in parallel. While the proliferation of astrocytes was noted in almost all lesions, it did not accompany neuronal loss in some regions, and spongiform changes were not apparent in the brain stem in most cases except for in the quadrigeminal plate and substantia nigra. Whereas spongiform changes in CJD are generally regarded an early event which precedes neuronal loss and astrocytosis,[4] astrocytosis was observed to occur before the appearance of spongiform changes in experimentally transmitted scrapie.[16] The proliferation of hypertrophic astrocytes therefore might not simply be a secondary change. (It should be also noted that the intensity of immunoreactivity against PrP did not parallel the histopathological alterations. In many regions, for example the pontine tegmentum and inferior olivary nucleus, the deposition of PrP was noted without accompanying spongiform changes or neuronal loss. This might indicate that these brain stem structures are resistant to the pathological processes induced by PrP.)

2 In the mesencephalon, the superior and inferior colliculi are consistently vulnerable in sporadic CJD, and similar involvement of the quadrigeminal plate was previously noted by some authors.[4] While the substantia nigra was affected in most cases, the changes were relatively mild. A few senile plaques were found in the periaqueductal gray matter in one case (case 1). Although the occurrence of amyloid plaques with a wide morphological spectrum has been previously documented in the mesencephalon of some cases of sporadic CJD,[5] the plaques in our case were immunohistochemically negative for PrP and probably represented a senile change.

3 The formation of large vacuoles in the perikarya of neurons has previously been consistently observed in the brain stem, especially in the medulla oblongata, in BSE[9,17] and scrapie,[8] and is pathognomonic for these disorders. Perikaryal vacuole formation is not a prominent feature in the cerebral or cerebellar cortex in sporadic CJD. On the other hand, it is commonly observed in the brain stem in kuru.[6,7] In the present study, this was seen in the oculomotor nucleus in two cases and in the substantia nigra in another case, without being accompanied by neuronal loss.

4 In the pontine base, although spongiform changes of the neuropil were found in only two cases, neuronal loss with astrocytosis of moderate to marked degree was noted in the pontine nuclei in most. The deposition of PrP was also observed in five of eight cases. It is certain that the pontine nuclei are sites which are consistently affected by the pathological processes that occur in sporadic CJD, and this is in accordance with the observations of Tateishi *et al.*[5] Recently Iwasaki *et al.*[10] also described gross atrophy of the pontine base, neuronal loss and prominent PrP immunoreactivity in the pontine nuclei in most cases of sporadic CJD, and similar results were also obtained for variant CJD.[12]

The sizes of the perikarya of the remaining neurons in the pontine nuclei appeared to be generally reduced in our series. Because the sizes of the neuronal perikarya show considerable regional variation within the pontine nuclei,[18] a more strict quantitative study is needed to confirm this observation. Neurons of the pontine nuclei send their axons to the cerebellar granule cell layer and also receive many fibers from the broad regions of the cerebral cortex.[18] Therefore, the possibility is considered that the atrophy of the neuronal perikarya in the pontine nuclei was partly caused by anterograde and/or retrograde trans-synaptic degeneration, as suggested by Tateishi *et al.*[5]

5 The medulla oblongata was preserved in an approximately normal state histopathologically except for one case. In thalamic type of CJD, severe degeneration of the inferior olivary nucleus constantly occurs.[19,20] In the present series, no case of thalamic type CJD was included and degeneration of the inferior olivary nucleus was not noted. However, in spite of the absence of pathological neuronal loss, the deposition of PrP was consistently found in the inferior olivary nucleus.

In recent years, the variability of clinicopathological phenotypes in patients with sporadic CJD has been demonstrated to depend on a polymorphism at codon 129 of the *PrP* gene as well as a pattern on Western immunoblot analysis of PrP, and a new classification scheme based upon these data is widely being employed.[21] Because the present study is a retrospective one that was performed on archival autopsy materials, the results of molecular analysis of PrP and its gene were not available for most of the cases. This is a major limitation of our study, and an investigation for the correlation of the molecular characteristics of PrP and pathological findings of brain stem lesions in sporadic CJD should be performed in future studies. At this stage, very limited inference can be made on the genotypes of *PrP* in the present series. Judging from the fact that in more than 90% of the Japanese population codon 129 of the *PrP* gene is homozygous for methionine (MM type) and also judging from the clinicopathological features of each patient in our series (periodic synchronous discharge was observed on electroencephalogram in all patients), it is supposed that most of our cases 1–7 are probably the MM1 type.

The relationship between the histopathological and immunohistochemical findings of the brain stem and the duration of the clinical course is another problem that remains to be elucidated. In the present series, the severity of the histopathological findings and the regional distribution of the immunohistochemical reactivity of PrP varied from case to case, and we could not find a clear correlation between the duration of the clinical course and these findings in the brain stem lesions.

In summary, we showed that in sporadic CJD pathological alterations of variable degree were observed in the brain stem, in particular in the quadrigeminal plate and pontine nuclei, although spongiform changes were found only infrequently. The medulla oblongata did not show any significant histopathological lesions. The deposition of PrP was mainly observed in the quadrigeminal plate and pontine nuclei. We also noted this in the pontine tegmentum and inferior olivary nucleus, which appeared to be approximately normal by histopathological examination. The remaining problems include the relationships between these changes in the brain stem and the lesions in the cerebellum, the possibility of trans-synaptic degeneration of neurons in the pontine nuclei, the clinical significance of these brain stem lesions, and the reasons for the differences between the lesions of the brain stem in sporadic CJD and those in kuru or variant CJD.

REFERENCES

1. Budka H, Aguzzi A, Brown P *et al.* Neuropathological diagnostic criteria for Creutzfeldt-Jakob disease (CJD) and other human spongiform encephalopathies (prion diseases). *Brain Pathol* 1995; **5**: 459–466.
2. Ironside JW. Review. Creutzfeldt-Jakob disease. *Brain Pathol* 1996; **6**: 379–388.
3. Mizutani T, Okumura A, Oda M, Shiraki H. Panencephalopathic type of Creutzfeldt-Jakob disease. Primary involvement of the cerebral white matter. *J Neurol Neurosurg Psychiat* 1981; **44**: 103–115.
4. Masters CL, Richardson EP Jr. Subacute spongiform encephalopathy (Creutzfeldt-Jakob disease). The nature and progression of spongiform change. *Brain* 1978; **101**: 333–344.
5. Tateishi J, Sato Y, Ohta M. Creutzfeldt-Jakob disease in humans and laboratory animals. *Progr Neuropathol* 1983; **5**: 195–221.
6. Klatzo I, Gajdusek DC, Zigas V. Pathology of kuru. *Lab Invest* 1959; **8**: 799–847.
7. Hainfellner JA, Liberski PP, Guiroy DC *et al.* Pathology and immunocytochemistry of a kuru brain. *Brain Pathol* 1997; **7**: 547–553.
8. Wood JLN, McGill IS, Done SH, Bradley DR. Neuropathology of scrapie. A study of the distribution patterns of brain lesions in 222 cases of natural scrapie in sheep, 1982–1991. *Vet Rec* 1997; **140**: 167–174.
9. Wells GAH, Wilesmith JW. The neuropathology and epidemiology of bovine spongiform encephalopathy. *Brain Pathol* 1995; **5**: 91–103.
10. Iwasaki Y, Sobue G, Yoshida M, Hashizume Y. Neuropathological characteristics of brainstem lesions in sporadic Creutzfeldt-Jakob disease. *Brain Pathol* 2003; **13**: s149.

11. Will RG, Ironside JW, Zeidler M *et al.* A new variant of Creutzfeldt-Jakob disease in the UK. *Lancet* 1996; **347**: 921–925.
12. Ironside JW, Head MW, Bell JE, McCardle L, Will RG. Laboratory diagnosis of variant Creutzfeldt-Jakob disease. *Histopathol* 2000; **37**: 1–9.
13. Kitamoto T, Shin RW, Doh-ura K *et al.* Abnormal isoform of prion proteins accumulates in the synaptic structures of the central nervous system in patients with Creutzfeldt-Jakob disease. *Am J Pathol* 1992; **140**: 1285–1294.
14. Brown P, Kenney K, Little B *et al.* Intracerebral distribution of infectious amyloid protein in spongiform encephalopathy. *Ann Neurol* 1995; **38**: 245–253.
15. Mizusawa H, Hirano A, Llena JF. Involvement of hippocampus in Creutzfeldt-Jakob disease. *J Neurol Sci* 1987; **82**: 13–26.
16. Wiley CA, Burrrola PG, Buchmeier MJ *et al.* Immunogold localization of prion filaments in scrapie-infected hamster brains. *Lab Invest* 1987; **57**: 646–656.
17. Wells GAH, Hancock RD, Cooley WA, Richards MS, Higgins RJ, David GP. Bovine spongiform encephalopathy. Diagnostic significance of vacuolar changes in selected nuclei of the medulla oblongata. *Vet Rec* 1989; **125**: 521–524.
18. Carpenter MB, Sutin J. *Human Neuroanatomy*, 8th edn. Baltimore/London: Williams & Wilkins, 1983.
19. Mizusawa H, Ohkoshi N, Sasaki H, Kanazawa I, Nakanishi T. Degeneration of the thalamus and inferior olives associated with spongiform encephalopathy of the cerebral cortex. *Clin Neuropathol* 1988; **7**: 81–86.
20. Kornfeld M, Seelinger DF. Pure thalamic dementia with a single focus of spongiform change in cerebral cortex. *Clin Neuropathol* 1994; **13**: 77–81.
21. Parchi P, Castellani R, Capellari S *et al.* Molecular basis of phenotypic variability in sporadic Creutzfeldt-Jakob disease. *Ann Neurol* 1996; **39**: 767–778.

Surface Plasmon Resonance Analysis for the Screening of Anti-prion Compounds

Satoshi KAWATAKE,[a] Yuki NISHIMURA,[a] Suehiro SAKAGUCHI,[b] Toru IWAKI,[c] and Katsumi DOH-URA*,[a]

[a] *Department of Prion Research, Tohoku University; Sendai 980–8575, Japan:* [b] *Department of Molecular Microbiology and Immunology, Nagasaki University; Nagasaki 852–8523, Japan: and* [c] *Department of Neuropathology, Neurological Institute, Kyushu University; Fukuoka 812–8582, Japan.*

Received November 2, 2005; accepted January 24, 2006; published online January 27, 2006

The interaction of anti-prion compounds and amyloid binding dyes with a carboxy-terminal domain of prion protein (PrP121—231) was examined using surface plasmon resonance (SPR) and compared with inhibition activities of abnormal PrP formation in scrapie-infected cells. Most examined compounds had affinities for PrP121—231: antimalarials had low affinities, whereas Congo red, phthalocyanine and thioflavin S had high affinities. The SPR binding response correlated with the inhibition activity of abnormal PrP formation. Several drugs were screened using SPR to verify the findings: propranolol was identified as a new anti-prion compound. This fact indicates that drug screenings by this assay are useful.

Key words anti-prion compound; surface plasmon resonance; scrapie-infected cell; screening; recombinant prion protein

Transmissible spongiform encephalopathies or prion diseases are fatal neurodegenerative disorders that include Creutzfeldt–Jakob disease and Gerstmann–Sträussler–Scheincker syndrome in humans, and scrapie, bovine spongiform encephalopathy and chronic wasting disease in animals. These disorders are characterized by accumulation in the brain of an abnormal isoform of prion protein (PrP), which includes a high beta-sheet content and is resistant to digestion with proteinase K.[1] Recent outbreaks of variant Creutzfeldt–Jakob disease[2] and iatrogenic Creutzfeldt–Jakob disease through use of cadaveric growth hormone or dura grafts[3] in younger people have necessitated the development of suitable therapies. Compounds such as antimalarials and amyloid binding dyes are known to possess anti-prion activity *in vitro* or *in vivo*.[4—14] Among them, Congo red and quinacrine are known to bind directly to PrP and thereby strongly inhibit proteinase K-resistant PrP (PrPres) formation.[15,16] However, it remains unclear whether or not other anti-prion compounds and amyloid binding dyes interact directly with PrP. This study analyzed interactions of some previously reported anti-prion compounds[4,7,11,17,18] and popularly used amyloid binding dyes with recombinant PrP using surface plasmon resonance (SPR). In addition, we evaluated whether SPR assay is useful as a screening tool for anti-prion compounds.

MATERIALS AND METHODS

Compounds Compounds used in the study (Fig. 1) were obtained from Sigma Aldrich Corp. (quinacrine dihydrochloride (QC, MW: 400.0), quinine hydrochloride (QN, MW: 324.4), thioflavin T (ThT, MW: 283.4, dye content 65%), thioflavin S (ThS, MW: undetermined), propranolol (MW: 295.8), promethazine hydrochloride (MW: 284.4), carbamazepine (MW: 236.3) and theophylline (MW: 180.2)), Aldrich (chloroquine diphosphate (CQ, MW: 319.9), and Congo red (CR, MW: 696.7, dye content 97%)), ICN (phthalocyanine tetrasulfonate (PcTS, MW: 922.7)), Wako Pure Chemical Industries Ltd. (Tokyo, Japan) (tetracycline hydrochloride (TC, MW: 444.4), diazepam (MW: 284.7), folic acid (MW: 441.4) and phenytoin (MW: 252.3)) or Nacalai Tesque (Tokyo, Japan) (testosterone (MW: 288.4)). All compounds were prepared as 20 mM stock solutions in water or dimethyl sulfoxide.

SPR Analysis The SPR analysis was performed using an

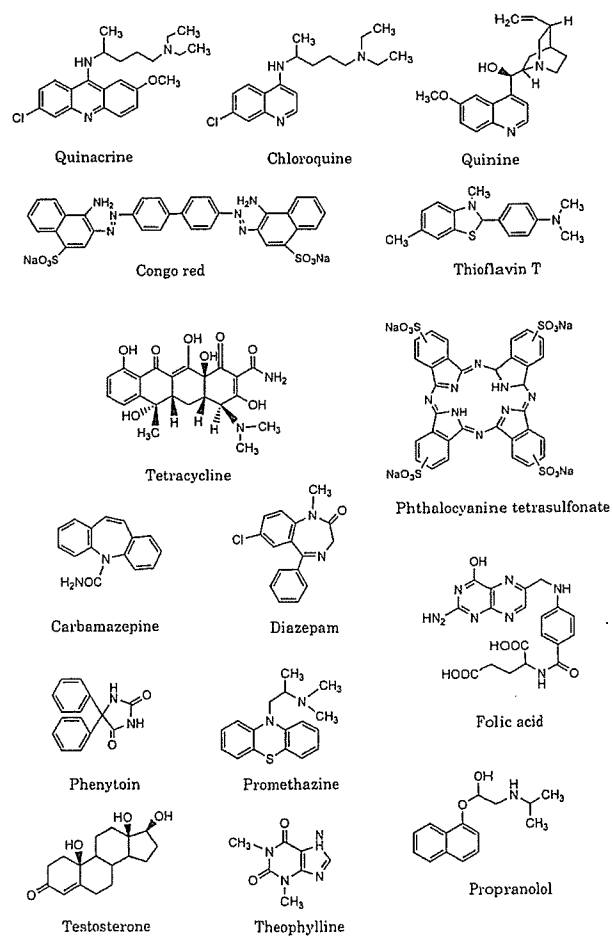

Fig. 1. Structures of Compounds or Drugs Used in the Study

* To whom correspondence should be addressed. e-mail: doh-ura@mail.tains.tohoku.ac.jp

optical biosensor (Biacore AB, Uppsala, Sweden) equipped with a CM5 sensor chip. Recombinant mouse PrP was prepared as described previously[19,20] and immobilized on a biosensor chip at a density of *ca.* 3000 resonance units (RU) using amine coupling.[21] Test compounds were diluted to 100 μM with running buffer (70 mM NaCl, 53 mM Na_2HPO_4, 12.5 mM KH_2PO_4, pH 7.4) and contained 0.5% DMSO. After they were confirmed to be in solution without precipitation or aggregation, they were injected over the PrP flow cell and the reference for either 60 s at a flow rate of 20 μl/min (low-affinity compounds) or 90 s at a flow rate of 30 μl/min (high-affinity compounds). The dissociation phase was monitored for 60 s (low-affinity compounds) or 270 s (high-affinity compounds). The flow cell was washed with 10 mM NaOH or 0.01% Triton X-100 for 30 s between each sample injection. Buffer blanks for double referencing were injected before sample analyses.[22]

The full-length recombinant of mouse PrP (residues 23—231) was used initially in the experiment, but it was easily degraded during SPR analysis in the amino-terminal portions attributable to an unidentified mechanism. For that reason, the carboxy-terminal polypeptide (residues 121—231; PrP121—231), which represents the only autonomous folding unit of PrP with a defined three-dimensional structure,[19,23,24] was used in this study.

Every PrP-immobilized biosensor chip used in the study was confirmed to respond almost the same and was standardized by the measurement of QC before its use for sample analyses.

Data Analysis The binding response, which is an index for estimating the interaction of a compound with molecules sited on a biosensor chip, is obtained from the equilibrium response (R_{eq}) value or the maximum response value in the sensorgram divided by the molecular weight.[25] In this study, the binding response of a compound was standardized by calibrating with QC, whose binding response was designated as 100 RU/Da. For low-affinity compounds, the dissociation constant (K_D) based on the R_{eq} state was calculated from data at doses ranging from 10 μM to 1 mM by either steady-state analysis using BIAevaluation software (ver. 3.0; Biacore AB) or Scatchard plot analysis. On the other hand, the K_D for high-affinity compound CR or PcTS was deduced after the data were fit to a binding model assuming a bivalent analyte in BIAevaluation software. The fitting was performed in such a way that the χ^2 value representing the statistical closeness of curve-fitting became the lowest. It was recommended ideally to be below 10.

Statistical linear correlation was evaluated using Pearson's correlation coefficient; Fisher's r to z method was used to calculate the p values. Simple linear regression analysis was also performed.

Anti-prion Activity Assay Anti-prion activity of a compound was assayed by measuring its 50% inhibition doses (IC_{50}) for PrPres formation in scrapie-infected neuroblastoma (ScNB) cells as described in previous reports.[7,11,12] Briefly, compounds were added at designated concentrations to the medium when cells were passed at 10% confluency. Cells were allowed to grow to confluence and lysed with lysis buffer (0.5% sodium deoxycholate, 0.5% Nonidet P-40, PBS). Lysates were digested with 10 μg/ml proteinase K for 30 min and centrifuged at 100000×g for 30 min at 4 °C. The pellets were resuspended in sample loading buffer and boiled. Samples were separated using electrophoresis on a 15% Tris-glycine-SDS-polyacrylamide gel and electroblotted. PrPres was detected using an antibody SAF83 (1 : 5000; SPI-Bio, France), followed by an alkaline phosphatase-conjugated secondary antibody. Immunoreactive signals were visualized using CDP-Star detection reagent (Amersham Biosciences Corp., U.S.A.) and were analyzed densitometrically. Three independent assays were performed in each experiment.

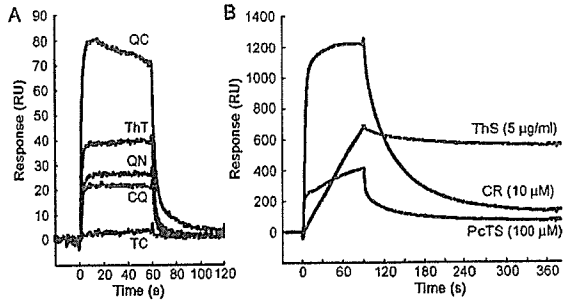

Fig. 2. Interactions of Anti-prion Compounds with PrP121—231

(A) Sensorgrams of the low-affinity compounds quinacrine (QC), chloroquine (CQ), quinine (QN), thioflavin T (ThT) and tetracycline (TC), all at 100 μM. (B) Sensorgrams of the high-affinity compounds Congo red (CR, 10 μM), phthalocyanine tetrasulfonate (PcTS, 100 μM) and thioflavin S (ThS, 5 μg/ml).

RESULTS

Interaction of Anti-prion Compounds with PrP The SPR sensorgrams of ThT and antimalarials such as QC, QN and CQ (each at 100 μM) demonstrated weak signal responses of less than 100 RU (Fig. 2A). The responses of these compounds reached equilibrium (R_{eq}) within a few seconds and returned to the baseline very rapidly after dissociation. These sensorgrams were typical for low-affinity interactions: TC showed almost no response. On the other hand, all sensorgrams of high-affinity compounds, such as CR, PcTS and ThS, showed much stronger responses and individual characteristic curves that differed from those of the low-affinity compounds (Fig. 2B). The CR (10 μM) showed the strongest signal, which was greater than 1200 RU: this decreased very slowly in the dissociation phase. The signal responses for PcTS (100 μM) and ThS (5 μg/ml) showed that neither reached the R_{eq} state within the association phase or returned to the baseline within the dissociation phase. In particular, ThS was only slightly dissociated and remained bound. This sensorgram resembled the sensorgram of biquinoline, an effective inhibitor of PrPres formation in ScNB cells (IC_{50}=3 nM).[11]

K_D Determination The dose response curve for QC appeared to be monophasic and to reach a saturation level at higher concentrations; its dissociation constant (K_D) value was calculated as 1.1 mM or 0.9 mM using steady-state analysis or Scatchard plot analysis, respectively (Figs. 3A—C). Vogtherr *et al.*[16] reported the dissociation constant (K_D= 4.6 mM) of the complex of QC and human PrP 121—230 analyzed by nuclear magnetic resonance (NMR) spectroscopy. This value was almost comparable to the K_D value obtained in this study, indicating that the method used in this study was relevant. The other two low-affinity compounds, QN and

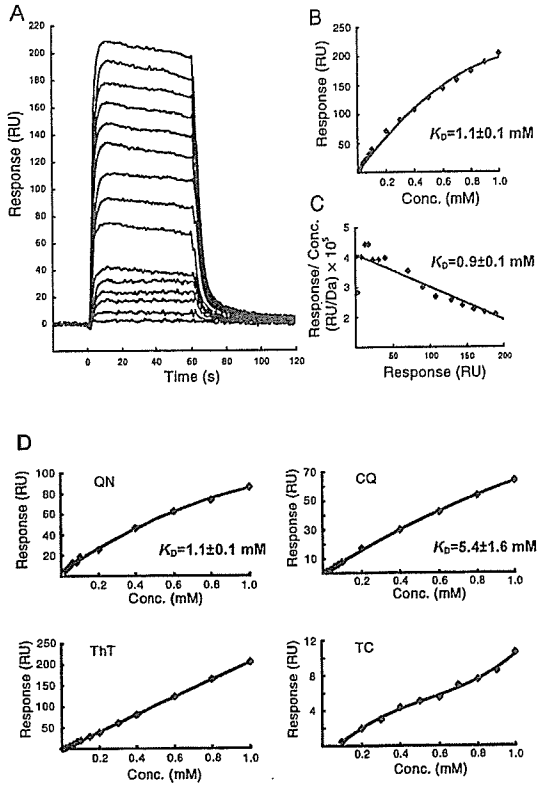

Fig. 3. Kinetic Analyses of Low Affinity Compounds

(A) Sensorgrams, (B) dose response curve and (C) scatchard plot of QC. (D) Dose response curves of QN, CQ, ThT, and TC.

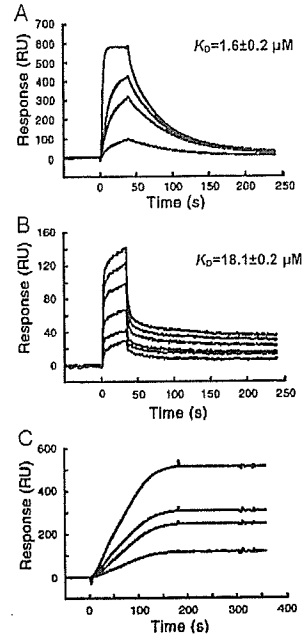

Fig. 4. Kinetic Analyses of High Affinity Compounds

(A) Sensorgrams of CR at concentrations of 1, 2, 3.3 and 5 μM, and its K_D value. (B) Sensorgrams of PcTS at concentrations of 1, 5, 10, 50, 75 and 100 μM, and its K_D value. (C) Sensorgrams of ThS at concentrations of 1, 2, 3 and 5 μg/ml, and its K_D value could not be calculated because of its undetermined structure and molecular weight.

CQ, respectively showed a similar monophasic pattern in dose response curves, yielding K_D of 1.1 mM and 5.4 mM (Fig. 3D). These K_D values, however, were of rough estimation and might be a little underscored due to lack of the data at concentrations of more than 1 mM. Unstable solubility of the compounds at such high concentrations hindered further analyses.

On the other hand, ThT gave a linear dose–response curve within a concentration of up to 1 mM and TC showed a biphasic pattern (Fig. 3D). Therefore, the saturation levels and K_D values of these compounds could not be determined, indicating that these compounds have a very low or no affinity with PrP121—231. Of them, TC is known to revert abnormal physicochemical properties of PrPres *in vitro*,[18] and interaction between TC and human PrP 106—126 peptides is revealed by NMR analysis.[26] Their data appear to be inconsistent with the data in this study. However, this discrepancy might be attributable to the lack of a TC binding site in the PrP121—231 used in our study.

Each sensorgram of high affinity compounds showed a very slow dissociation phase and was individually characteristic (Fig. 4). The structural and stoichiometric binding details of the compounds with PrP121—231 have not yet been established, but CR or PcTS is a symmetrical molecule and either half of the molecule has anti-prion activity (Doh-ura K, unpublished data). Consequently, the K_D value for the compound was deduced after the data were fit to a binding model assuming a bivalent analyte. The K_D of CR was calculated to be 1.6 μM from the sensorgrams of 1, 2, 3.3 and 5 μM (χ^2=20.9±2.1) (Fig. 4A). The K_D of PcTS was calculated as 18.1 μM from the sensorgrams of 1, 5, 10, 50, 75 and 100 μM (χ^2=28.1±2.9) (Fig. 4B). The K_D of ThS was incalculable to an exact degree because it is presumed to be a mixture of compounds formed by methylation and sulfonation of primulin; their structures and molecular weights have not been determined.

Comparison between PrP Affinity and Anti-prion Activity The IC_{50} value for the inhibition of PrPres formation in ScNB cells, either previously reported or examined in this study, was used as an anti-prion activity in this study. It was compared with the K_D or with the binding response. The latter, an index for estimating the interaction, was obtained from the R_{eq} value or the maximum response value at a concentration of 1 mM divided by the molecular weight (Table 1).

From data of all compounds except ThT, TC and ThS, statistical analyses demonstrated a significant linear correlation between the reciprocal of binding response and the IC_{50} (r=0.985, p=0.0005) (Fig. 5). This relation appeared to be also observed in TC, but not in ThT showing the next highest binding response to QC but no inhibition of PrPres formation within a non-toxic dose range. However, ThT demonstrated cell-toxicity at such a low dose as 0.05 μM.

For ThS, assuming that its minimum molecular weight deduced from presumable structures was 520 Da, its binding response was estimated to be 5.03 RU/Da; the IC_{50} was estimated to be about 2 μM, corresponding to about 1 μg/ml. However, these values seem to be underestimates because some constituents of ThS might interact with PrP121—231 or have inhibitory activity for PrPres formation. Therefore, active constituents of ThS might be expected to inhibit PrPres formation in ScNB cells at a submicromolar dose, similar to the other high-affinity compounds.

Screening by SPR Findings suggested that a compound

Table 1. Binding Response, Dissociation Constant (K_D) and 50% PrPres Inhibition Dose in ScNB Cells (IC_{50})

Compound	Binding response[a] (RU/Da)	K_D[b] (mM)	IC_{50}[c] (μM)
Low-affinity			
Quinacrine (QC)	0.25±0.00	1.1±0.1 (0.9±0.1)	0.3 (7)
Quinine (QN)	0.05±0.00	1.1±0.1 (1.4±0.1)	6.0 (11)
Chloroquine (CQ)	0.07±0.01	5.4±1.6 (3.5±0.8)	4.0 (7)
Thioflavin T (ThT)	0.16±0.01	n.d.[d] (n.d.[d])	No effect[f]
Tetracycline (TC)	0.01±0.00	n.d.[d] (n.d.[d])	No effect[g]
High-affinity			
Congo red (CR)	8.74±0.64	$1.6\pm0.2\times10^{-3}$	1.5×10^{-2} (4)
Phthalocyanine tetrasulfonate (PcTS)	1.82±0.06	$18.1\pm0.2\times10^{-3}$	0.5 (17)
Thioflavin S (ThS)	n.d.[e]	n.d.[e]	*ca.* 1 μg/ml

a) Binding response value was calculated from the R_{eq} value divided by the molecular weight for QC, QN, CQ and CR, or from the response value at a concentration of 1 mM divided by the molecular weight for ThT, TC and PcTS. *b*) K_D values were determined by steady state analysis for the low-affinity compounds or by bivalent analyte model analysis for CR and PcTS. K_D values from Scatchard plot analyses are shown in parentheses. *c*) IC_{50} values reported in the literature (reference shown in parentheses) or examined in this study. *d*) n.d.: not determined because a saturation level could not be estimated. *e*) n.d.: not determined because its structure and molecular weight were undetermined. *f*) Inhibition of PrPres formation was not observed up to a minimal toxic dose of 0.05 μM. *g*) Inhibition of PrPres formation was not observed up to a minimal toxic dose of 5.0 μM.

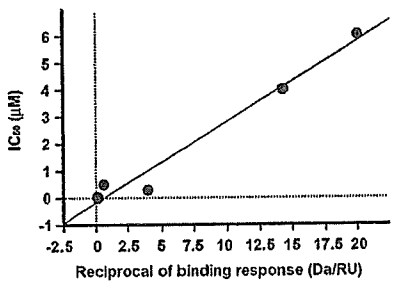

Fig. 5. Correlation between the Reciprocal of Binding Response and the IC_{50}

The data were from five compounds in which both binding response and IC_{50} were determined. Correlation showed a slope of 0.298, an intercept of −0.156 and a correlation coefficient of 0.971 (p=0.002) by simple linear regression analysis.

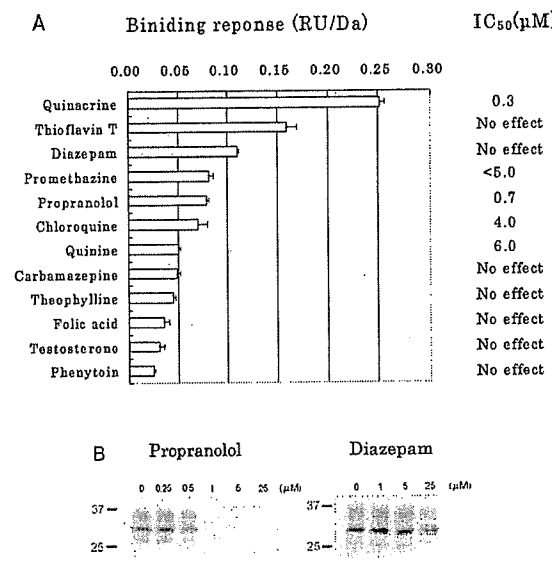

Fig. 6. Screening of Anti-prion Candidates Using the SPR Assay

(A) Binding response of each sample at 100 μM, and its IC_{50} of PrPres formation inhibition in ScNB cells within a non-toxic dose range. (B) Inhibition analyses of PrPres formation in ScNB cells grown in the presence with propranolol or diazepam. Molecular sizes in kDa are shown at the left of each panel.

capable of interacting with PrP121—231 might have a potency of inhibiting PrPres formation in ScNB cells. To verify this inference, several drugs were examined for either their binding response using the SPR method or their IC_{50} in ScNB cells. Eight clinically utilized drugs—carbamazepine, diazepam, folic acid, phenytoin, promethazine, propranolol, testosterone, and theophylline—all of which are low molecular weight compounds capable of crossing the blood brain barrier and share a partial structure similarity with the anti-prion compounds already reported, were examined and compared with the four anti-prion compounds (QC, QN, CQ, and ThT) (Fig. 6A).

Diazepam, promethazine and propranolol showed a higher binding response value than QN, which was the lowest binding response compound among the effective anti-prion compounds examined in this study. Among these, promethazine or propranolol inhibited PrPres formation in ScNB cells (propranolol: IC_{50}=0.7 μM; promethazine: IC_{50}<5.0 μM). Promethazine has already been reported to have anti-prion activity in ScNB cells,[8] whereas propranolol is a novel compound that inhibits PrPres formation in ScNB cells. Diazepam apparently did not inhibit PrPres formation within a non-toxic dose range up to 25 μM (Fig. 6B). Inhibitory activities against PrPres formation in ScNB cells were not observed for other drugs that had lower binding response values than QN.

DISCUSSION

We demonstrated that most anti-prion compounds examined in this study interacted with PrP121—231. The binding response of the compounds correlated with the IC_{50} of PrPres formation inhibition in ScNB cells. In addition, based on this finding, we proved that this interaction analysis using the SPR method was useful for screening to identify new candidates of anti-prion compounds. Three different *in vitro*

screening assays have been reported recently. One is yeast based,[27] one uses ScN2a cells,[10] and the other is based on fluorescence correlation spectroscopy.[28] These assays are suitable for high-throughput screening of large compound libraries to identify novel lead molecules. The SPR method reported here, which easily assayed interactions between compounds and PrP molecules within less than 3 min per compound, is applicable to high-throughput *in vitro* assay for screening of large compound libraries if more highly performing SPR machines are used. The usefulness of this method in screening for PrP binding ligands is also reported very recently by other researchers.[29]

Two chemicals, ThT and diazepam, showed high binding response but did not inhibit PrPres formation within a non-toxic dose range. Of them, ThT exhibited very low or no affinity with PrP121—231 but the next highest binding response to QC. This suggests that ThT might interact with PrP121—231 non-specifically. For diazepam, similar non-specific interaction with PrP121—231 might be occurred, or the interaction might be specific but unrelated to conversion to PrPres. These inferences, however, remain unsupported by other experimental results obtained here.

On the other hand, such high-affinity compounds as CR and PcTS showed large amounts of binding to PrP121—231. One possible interpretation for this is that the compounds might have two or more binding sites per molecule. In fact, structure–activity relationship analysis for these symmetrical compounds indicates that either half of the molecule has anti-prion activity (Doh-ura K, unpublished data), and their sensorgrams looked very similar to those of anti-PrP antibodies (data not shown). The other is that the compounds might self-assemble to interact with the PrP molecule. It has long been known that CR and many other bis-azo dyes self-assemble in water solutions, and this property is proposed to associate with binding capability.[30]

Instead of the full length of mouse PrP, a carboxy-terminal domain of mouse PrP (PrP121—231) was used in the study because of instability of the full length PrP during the experiment. This carboxy-terminal domain is the only autonomous folding unit of PrP with a defined three-dimensional structure[19,23,24] and contains epitopes recognized by a majority of antibodies bearing anti-prion activity.[31—37] Taken together with our findings suggesting that most of anti-prion compounds might exert their effects by interacting with this domain, targeting the carboxy-terminal domain should not necessarily be either inefficient or inappropriate for looking for new anti-prion compounds.

In conclusion, our study indicated that most anti-prion compounds tested here interacted with and had an affinity for recombinant PrP121—231. The SPR binding response to the PrP121—231 correlated with the anti-prion activity in ScNB cells. These observations will allow further discovery of new classes of anti-prion compounds using the SPR assay.

Acknowledgements This study was supported by grants to K.D. from the Ministry of Health, Labour and Welfare (H16-kokoro-024) and the Ministry of Education, Culture, Sports, Science and Technology (14021085), Japan. The authors thank Dr. Kenta Teruya for critical review of the manuscript.

REFERENCES

1) Prusiner S. B., *Science*, **252**, 1515—1522 (1991).
2) Will R. G., Ironside J. W., Zeidler M., Cousens S. N., Estibeiro K., Alperovitch A., Poser S., Pocchiari M., Smith P. G., *Lancet*, **347**, 921—925 (1996).
3) Brown P., Preece M., Brandel J. P., Sato T., McShane L., Zerr I., Fletcher A., Will R. G., Pocchiari M., Cashman N. R., d'Aignaux J. H., Cervenakova L., Fradkin J., Schonberger L. B., Collins S. J., *Neurology*, **55**, 1075—1081 (2000).
4) Caughey B., Race R. E., *J. Neurochem.*, **59**, 768—771 (1992).
5) Demaimay R., Chesebro B., Caughey B., *Arch. Virol. Suppl.*, **16**, 277—283 (2000).
6) Rudyk H., Vasiljevic S., Hennion R. M., Birkett C. R., Hope J., Gilbert I. H., *J. Gen. Virol.*, **81**, 1155—1164 (2000).
7) Doh-ura K., Iwaki T., Caughey B., *J. Virol.*, **74**, 4894—4897 (2000).
8) Korth C., May B. C., Cohen F. E., Prusiner S. B., *Proc. Natl. Acad. Sci. U.S.A.*, **98**, 9836—9841 (2001).
9) Ryou C., Legname G., Peretz D., Craig J. C., Baldwin M. A., Prusiner S. B., *Lab. Invest.*, **83**, 837—843 (2003).
10) Kocisko D. A., Baron G. S., Rubenstein R., Chen J., Kuizon S., Caughey B., *J. Virol.*, **77**, 10288—10294 (2003).
11) Murakami-Kubo I., Doh-ura K., Ishikawa K., Kawatake S., Sasaki K., Kira J., Ohta S., Iwaki T., *J. Virol.*, **78**, 1281—1288 (2004).
12) Ishikawa K., Doh-ura K., Kudo Y., Nishida N., Murakami-Kubo I., Ando Y., Sawada T., Iwaki T., *J. Gen. Virol.*, **85**, 1785—1790 (2004).
13) Poli G., Martino P. A., Villa S., Carcassola G., Giannino M. L., Dal-l'Ara P., Pollera C., Iussich S., Tranquillo V. M., Bareggi S., Mantegazza P., Ponti W., *Arzneim-Forsch.*, **54**, 406—415 (2004).
14) Sellarajah S., Lekishvili T., Bowring C., Thompsett A. R., Rudyk H., Birkett C. R., Brown D. R., Gilbert I. H., *J. Med. Chem.*, **47**, 5515—5534 (2004).
15) Caughey B., Brown K., Raymond G. J., Katzenstein G. E., Thresher W., *J. Virol.*, **68**, 2135—2141 (1994).
16) Vogtherr M., Grimme S., Elshorst B., Jacobs D. M., Fiebig K., Griesinger C., Zahn R., *J. Med. Chem.*, **46**, 3563—3564 (2003).
17) Caughey W. S., Raymond L. D., Horiuchi M., Caughey B., *Proc. Natl. Acad. Sci. U.S.A.*, **95**, 12117—12122 (1998).
18) Forloni G., Iussich S., Awan T., Colombo L., Angeretti N., Girola L., Bertani I., Poli G., Caramelli M., Grazia Bruzzone M., Farina L., Limido L., Rossi G., Giaccone G., Ironside J. W., Bugiani O., Salmona M., Tagliavini F., *Proc. Natl. Acad. Sci. U.S.A.*, **99**, 10849—10854 (2002).
19) Hornemann S., Glockshuber R., *J. Mol. Biol.*, **261**, 614—619 (1996).
20) Liemann S., Glockshuber R., *Biochemistry*, **38**, 3258—3267 (1999).
21) Johnsson B., Lofas S., Lindquist G., *Anal. Biochem.*, **198**, 268—277 (1991).
22) Myszka D. G., *J. Mol. Recognit.*, **12**, 279—284 (1999).
23) Hornemann S., Korth C., Oesch B., Riek R., Wider G., Wuthrich K., Glockshuber R., *FEBS Lett.*, **413**, 277—281 (1997).
24) Riek R., Hornemann S., Wider G., Billeter M., Glockshuber R., Wuthrich K., *Nature* (London), **382**, 180—182 (1996).
25) Frostell-Karlsson A., Remaeus A., Roos H., Andersson K., Borg P., Hamalainen M., Karlsson R., *J. Med. Chem.*, **43**, 1986—1992 (2000).
26) Tagliavini F., Forloni G., Colombo L., Rossi G., Girola L., Canciani B., Angeretti N., Giampaolo L., Peressini E., Awan T., De Gioia L., Ragg E., Bugiani O., Salmona M., *J. Mol. Biol.*, **300**, 1309—1322 (2000).
27) Bach S., Talarek N., Andrieu T., Vierfond J. M., Mettey Y., Galons H., Dormont D., Meijer L., Cullin C., Blondel M., *Nat. Biotechnol.*, **21**, 1075—1081 (2003).
28) Bertsch U., Winklhofer K. F., Hirschberger T., Bieschke J., Weber P., Hartl F. U., Tavan P., Tatzelt J., Kretzschmar H. A., Giese A., *J. Virol.*, **79**, 7785—7791 (2005).
29) Touil F., Pratt S., Mutter R., Chen B., *J. Pharm. Biomed. Anal.*, **40**, 822—832 (2006).
30) Skowronek M., Roterman I., Konieczny L., Stopa B., Rybarska J., Piekarska B., *J. Comput. Chem.*, **21**, 656—667 (2000).
31) Horiuchi M., Caughey B., *EMBO J.*, **18**, 3193—3203 (1999).
32) Heppner F. L., Musahl C., Arrighi I., Klein M. A., Rulicke T., Oesch B., Zinkernagel R. M., Kalinke U., Aguzzi A., *Science*, **294**, 178—182 (2001).
33) Enari M., Flechsig E., Weissmann C., *Proc. Natl. Acad. Sci. U.S.A.*, **98**, 9295—9299 (2001).

34) Peretz D., Williamson R. A., Kaneko K., Vergara J., Leclerc E., Schmitt-Ulms G., Mehlhorn I. R., Legname G., Wormald M. R., Rudd P. M., Dwek R. A., Burton D. R., Prusiner S. B., *Nature* (London), **412**, 739—743 (2001).
35) White A. R., Enever P., Tayebi M., Mushens R., Linehan J., Brandner S., Anstee D., Collinge J., Hawke S., *Nature* (London), **422**, 80—83 (2003).
36) Féraudet C., Morel N., Simon S., Volland H., Frobert Y., Créminon C., Vilette D., Lehmann S., Grassi J., *J. Biol. Chem.*, **280**, 11247—11258 (2005).
37) Miyamoto K., Nakamura N., Aosasa M., Nishida N., Yokoyama T., Horiuchi H., Furusawa S., Matsuda H., *Biochem. Biophys. Res. Commun.*, **335**, 197—204 (2005).

特集 アルツハイマー病―臨床医が診断後なすべきこと

認知症診断に役立つ補助検査法
―生物学的診断マーカーと脳分子イメージング

Diagnostic adjuncts of dementia ; Biomarker and molecular imaging

東北大学大学院医学系研究科先進漢方治療医学講座教授
Hiroyuki Arai 荒井啓行

東北大学大学院医学系研究科先進医工学研究機構教授
Yukitsuka Kudo 工藤幸司

Summary

補助検査法として，CTまたはMRIによる画像検査は水頭症や硬膜下血腫との鑑別診断および脳腫瘍の発見のため必須の検査である。認知症医療においては，早期診断をサポートするための検査法が最も重要であるが，そのなかで将来の予防医学を見据えたアミロイドの沈着を画像化する分子イメージングが注目を集めている。日本は独自に開発した分子イメージング技術を世界に向けて発信すべきであり，米国で開発されたPIB-PETを導入するだけではあまりに安易すぎる。

Key words

●アルツハイマー病
●バイオマーカー
●脳分子イメージング
●タウ蛋白
●アミロイド
●予防医学

I はじめに

一般に，認知症とは「一度獲得された知的機能の後天的な障害によって，自立した日常生活機能を喪失した状態」と定義されることが多い。より操作的な米国のアルツハイマー病(Alzheimer's disease；AD)の臨床診断基準であるNINCDS-ADRDA(National Institute of Neurological and Communicative Disorders and Strokes-the Alzheimer's Disease and Related Disorders Association)[1]やDSM-Ⅳ(Diagnostic and Statistical Manual of Mental Disorders-Ⅳ)でも，「記憶障害のみならず，失語，失行，実行機能障害などがみられ，複数の脳領域にまたがって高次機能が障害された結果として，以前の日常生活機能レベルからダウンし自立した生活が維持できない」ことが確認されてはじめて認知症と診断されることになっている。このNINCDS-ADRDAの基準でprobable AD(臨床的に確実なAD)と診断された症例を剖検し，その病理診断をゴールドスタンダードとして比較研究した結果が報告されているが，臨床診断と病理診断の一致率はほぼ80%と高い。認知症の診断はあくまで臨床医の目でみた医学的判断であり，繁用される改訂長谷川式簡易知能評価スケールやMMSE(mini-mental state examination)で○○点以下が認知症というものでもない。診断に重要なポイントは，以前のレベルからの低下＝declineである。かつては何でもできた人が，字も書

けなくなった，服も1人では着られないといった進行したケースであれば，認知症の判断は比較的容易であろう。しかし，「最近物忘れが目立つ」といった場合，年齢のためなのか，環境要因なのか，あるいは認知症のはじまりなのかの判断は臨床的観察のみでは非常に困難である。現に，昨年受診したA病院では「年のせい」と診断されたが，今年受診したB病院では「ADの初期」との診断を受け，困惑顔でセカンド(サード)オピニオンを求めてくることも多い。特にこの傾向は，塩酸ドネペジルが本格的に使われはじめた2000年以降顕著となり，「早期治療のための早期診断」を求める声として広がっている。本稿のテーマである「認知症診断に役立つ補助検査法」とは，このような早期診断をサポートする臨床検査法としての意義が最も期待されている。2001年 American Academy of Neurology から出された認知症診断の practice parameter[2]を参照されたい。ADに関してはNINCDS-ADRDA を用いての probable AD[1]，クロイツフェルト-ヤコブ病では Brown の診断基準[3]を用いることがガイドラインとされ，レビー小体病は McKeith らの consortium 診断基準[4]，前頭側頭型認知症(frontotemporal dementia)では Lund-Manchester の consortium 診断基準[5]を用いることが有用(option)とされている。血管性認知症(vascular dementia；VD)に関しては診断基準の推奨はせず，Hachinski の虚血スコア[6]を option として挙げている。この practice parameter の結論として，バイオマーカーの開発とその validation がきわめて重要であること，そして理想的なバイオマーカーやイメージングは認知症発症前に検出能力を有するものでなければならないことが強調されている。

Ⅱ 鑑別診断のための CT または MRI による画像診断は必須である

CT または MRI による画像診断は必須の検査であるが，造影まではルーチンの検査では行わない。画像診断はラクナー梗塞や大脳白質病変の検出に有用であるばかりでなく，水頭症や硬膜下血腫など脳外科領域の治療可能な認知症(treatable dementia)の発見に直接結びつく。ときに脳腫瘍や血管奇形が発見されることもある。脳萎縮の解釈は難しい。脳萎縮があっても認知面では全く正常という場合もあり，逆にADの初期段階では全く脳萎縮がみられないこともあり，脳萎縮を診断の拠り所にしてはいけない。また，陳旧性の血管病変(cerebrovascular disease；CVD)はVDの必要条件であるが，血管病変があればVDと短絡的に診断してはならない。現在の認知機能低下がCT/MRIで示された血管病変の部位・大きさから説明可能な妥当性を有するものであるかどうかの慎重な判断が要求される。高齢になるにつれ無症候性脳梗塞や大脳白質病変の頻度が増加する。高齢者ADの約3分の1にラクナー梗塞がみられるが，これをどのように扱うかは問題の残るところである。これをAD with CVD(あくまで中心はADであり付随的に血管障害を考える)とする立場と mixed dementia(血管障害もADもともに認知機能の低下に寄与する)とする立場があるが，少なくとも短絡的にVDとしないような注意深さは必要であろう。ADとVDの鑑別では，画像所見はあくまで参考であり1人1人の患者の臨床経過や全体像を総合的に評価すべきである。その際，前述の随伴する局所神経症状の有無を含めHachinskiの虚血スコアが重要な参考となることもある[6]。SPECTやPETなどの機能画像法は，局所脳機能を知るのに有用である。ADでは典型的には側頭頭頂葉領域で，レビー小体を伴う認知症では側頭頭頂葉領域に加えて後頭葉で，進行性核上性麻痺では前頭葉で，皮質基底核変性症では前頭頭頂葉領域での血流や代謝の低下がみられる。梗塞巣が大脳基底核・内包付近の穿通枝領域に多発するタイプのVDでは，前方型の血流や代謝の低下を示すことが多い。

バイオマーカーとしては，脳脊髄液検査が有用である[7]。慢性化した中枢神経感染症や脱髄性疾患による認知症では髄液細胞数，蛋白濃度などに異常がみられる。最近われわれはADの約80～85%の症例では，神経原線維変化(neurofibrillary tangles；NFT)の形成と神経細胞死を反映して，その主要構成成分である(リン酸化)タウ蛋白が髄液中に流出する結果，髄液(リン酸化)タウ蛋白が高値を示すことを明らかにした。典型的なVDでは髄液(リン酸化)タウ蛋白は上昇せず，ADとは明らか

に差別化しうる。進行性核上性麻痺や皮質基底核変性症などのいわゆるタウオパチーでも髄液(リン酸化)タウ蛋白が上昇する症例もあり，上述のような機能画像所見や神経所見を勘案して判断する。さらに，髄液(リン酸化)タウ蛋白レベルは，ADに進行する軽度認知障害(mild cognitive impairment；MCI)の約85%においてベースラインですでに高値であり，早期診断として有用である。髄液アミロイドβ蛋白(Aβ)1-42レベルは，老人斑へのAβの蓄積を反映してADでは低下する。髄液は腰椎穿刺という侵襲的手段を用いてのみ採取可能であること，および一般高齢者のスクリーニング検査としては適さないことなどが欠点として挙げられるが，北欧諸国やドイツにおいて盛んに行われており，日本でも一部の専門外来で施行されている[7]。ADの診断に有用な血液や尿からのバイオマーカーは知られていない。クロイツフェルト-ヤコブ病における髄液14-3-3蛋白は，診断的価値が高いとされているが，早期診断にはMRI拡散強調画像において高信号域を検出する方法が優れている[8]。心不全に伴う認知機能低下やせん妄などの認知症様状態との鑑別のため，胸部X線写真，心電図，一般採血などの内科一般の検査は必須である。また症例によっては血清梅毒反応，ビタミンB_{12}や葉酸，甲状腺ホルモンの測定も行い，treatable dementiaの発見に努める。

検査項目ではないが，高齢者において特に重要なものとして，現在服用している薬物をきちんと聞くことを怠ってはならない[9]。高齢者では潜在的な腎機能低下のため，薬物の腎排泄が遅延しており，体内に蓄積しやすいため常用量でも副作用を招きやすい。認知機能低下や日中の傾眠・転倒傾向などの背景に抗不安薬，抗精神病薬，抗コリン作用をもった薬剤などがないか注意深く聞き出す必要がある。

Ⅲ 予防医学を見据えた新しい画像診断技術の開発 ―脳分子イメージング

AD脳においては，2つの重要な神経病理変化が観察される。老人斑とNFTである。前者は分子量4kDa程度のAβにより，後者は高度にリン酸化されたタウ蛋白により構成されている。図1に示すように，70歳から物忘れが目立つようになり5年ほどは日常生活が自立していたが，75歳時には問題行動が出現しADとの診断を受けた患者を想定すると，この患者ではAβの脳への蓄積が始まったのは50歳前後，NFT(タウ蛋白のリン酸化)とそれに伴う神経細胞死が始まったのが60～65歳前後と予想されるのである。年齢には多少の前後はあるにしても，ADではAβの蓄積開始から臨床的に認知症の初期症状が出現するまでに20年ものタイムラグがあることをまず認識しなければならない。70歳からAβの蓄積が始まった場合は，90歳にならないと認知症が顕在化しない。このような患者が仮に80歳で他の原因で死亡したとすると，Aβの広範な沈着はあるがタウは全く沈着していない非認知症老人ということになる。これは一見Aβと認知症発症のネガティブな関連を示すように思えるが，そうではない。つまり，何歳で認知症を発症するかは，何歳からAβが蓄積を開始するかで規定されると考えられる。平均寿命が60歳の時代と80歳の時代を考えてみよう。60歳までに認知症が顕在化するには，40歳かそれ以前にAβが蓄積を開始しなければならないが，このようなケースはきわめてまれであり，アミロイド前駆体遺伝子，

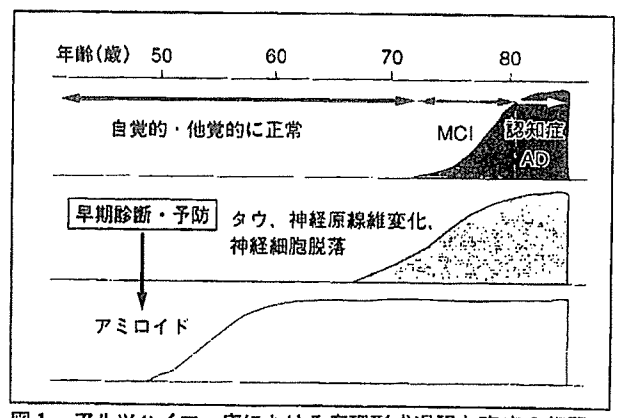

図1 アルツハイマー病における病理形成過程と臨床の相関
アミロイド沈着と臨床的な症状顕在化の間には20年以上の長い潜伏期間がある。この期間は完全に無症状であるが，抗アミロイド治療開始のゴールデンタイムでもある。
(井原康夫．平成15年度日本医学会シンポジウムより)

プレセニリン-1遺伝子，プレセニリン-2遺伝子の突然変異を伴う家系か，疾患感受性遺伝子であるアポリポ蛋白E4遺伝子の保有者に限られ，平均寿命60歳の時代には認知症はほとんどみられなかった。一方，平均寿命が80歳の時代では，60歳までにAβが蓄積を開始したケースが(他の原因で死亡しなければ)すべて上積みされることになり，認知症はよりcommon disease(ありふれた病気)となり社会に対するインパクトを変えていくことになる。東京都の1995年の調査でも，80歳台の認知症有病率は約20%，90歳台では約40%，100歳以上では実に約90%となっている。長生きすればするほど，水面下にあった病変が水面上に頭を出すこと，つまり認知症が顕在化することになる。これが，今日AD患者が増え続ける理由である。21世紀の日本は長寿と引き換えに認知症という重い荷物を背負うことになったといえる。このようなAβ蓄積を起点とし，その後のすべてのイベントをAβ蓄積から説明しようとする考え方を今日「アミロイド仮説」と呼んでいる。このアミロイド仮説は根本的な治療法の開発に向けての創薬の原点ともなっている。

東北大学先進医工学研究機構の工藤らは，入手可能な有機化合物ライブラリーから，蛋白化学的手法を用いて，凝集しβシート構造をとった老人斑Aβに「鍵」と「鍵穴」の関係のごとく結合するプローブの開発に成功した[10][11]。選択された化合物はさらに最適化され，放射ラベル化し，PETにて画像を得る。この方法により，ADを臨床像によらず，蓄積物質に基づき診断することが可能となる(図2)。また，①発症原因物質とみなされているAβやタウ蛋白に関するストレートな情報を有する，②繰り返し検査可能である，③Aβの蓄積を的確に把握でき，発症前診断が可能となる，④安全で有効なAβ生成・凝集阻害剤が開発されれば，ADの発症をコントロールすることが可能となるなど，さまざまな利点を有する。米国では，Pittsburgh compound B(PIB)というプローブを用いたアミロイド分子イメージングが早くも始まっている。米国では，このPIB-PETとアミロイドワクチン療法，あるいはγセクレターゼ阻害薬による臨床治験が抱き合わせで進行しているようである(ハーバード大学神経学Growdenからの私信)。2005年6月に米国で開催されたADの予防に関する国際会議で，ピッツバーグ大学のKlunkらによって図3のようなPIB-PET診断の進捗状況が報告されている。左の2名は正常コントロール，中央の3名はMCI，右の1名はADと臨床診断されたケースである。ADでAβが広範に蓄積していることは明らかであるが，注目すべきは，正常者でもAβ沈着が始まっていることが確認され，MCIに至っては，ADと同程度に沈着しているケースもあれば，全くAβが観察されないケースもあるということである。人間の目をはるかに超える感度をもつこのような技術開発が行われると，正常，MCIあるいはADなどという臨床診断の意味が根本から問い直されることになろう。Aβの蓄積の程度に基づいた新たな分類が生まれてくるかもしれない。一方，先述のGrowdenは2005年

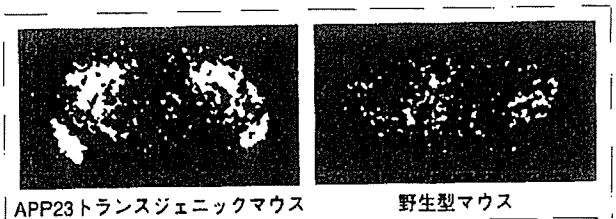

図2 [^{18}F]BF-168静注3時間後に摘出した脳標本のオートラジオグラフィー像(巻頭グラビアページ参照)
[^{18}F]BF-168を遺伝子改変マウス(APP23)に静注し，3時間後オートラジオグラフィーを撮った。[^{18}F]BF-168は遺伝子改変マウスの老人斑に結合している。

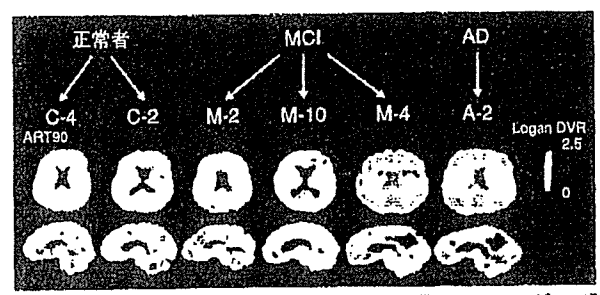

図3 PIB-PETを用いたヒトアミロイド分子イメージング(巻頭グラビアページ参照)
左の2名は正常コントロール，中央の3名はMCI，右の1名はADと臨床診断されたケースである。
(Klunk WE, et al. Alzheimer's Association/Prevention会議，2005.6より)

12月の第3回 Takeda Symposium で講演し，生前 PIB-PET 検査を受け陽性所見を示した患者の1例を提示し，剖検では陽性所見を示した側頭葉には全く老人斑はなく，血管アミロイド症のみであったことから，PIB-PET の解釈に慎重にならざるをえないと述べている。

理化学研究所理事長でノーベル化学賞を受賞した野依良治氏は，若く優秀な研究者を育成し，公共性を重視しつつ競争力のある技術開発を地道に行うことこそ国益に資する投資であると述べている(2006年1月6日付日本経済新聞)。日本は独自に開発した分子イメージング技術を世界に向けて発信すべきであり，米国で開発された PIB-PET を日本に導入するだけではあまりに安易すぎないだろうか。

文 献

1) McKhann G, Drachman D, Folstein M, et al : Clinical diagnosis of Alzheimer's disease ; Report of the NINCDS-ADRDA Work Group under the auspices of the Department of Health and Human Services Task Force on Alzheimer's Disease. Neurology 34 : 939-944, 1984
2) Knopman DS, DeKosky ST, Cummings JL, et al : Practice parameter ; Diagnosis of dementia (an evidence-based review). Report of the Quality Standards Subcommittee of the American Academy of Neurology. Neurology 56 : 1143-1153, 2001
3) Brown P, Cathala F, Castaigne P, et al : Creutzfeldt-Jakob disease ; Clinical analysis of a consecutive series of 230 neuropathologically verified cases. Ann Neurol 20 : 597-602, 1986
4) McKeith LG, Galasko D, Kosaka K, et al : Consensus guidelines for the clinical and pathologic diagnosis of dementia with Lewy bodies(DLB) ; Report of the consortium on DLB international workshop. Neurology 47 : 1113-1124, 1996
5) The Lund and Manchester Group : Clinical and neuropathological criteria for frontotemporal dementia. J Neurol Neurosurg Psychiatry 57 : 416-418, 1994
6) Hachinski VC, Lassen NA, Marshall J : Multi-infarct dementia ; A cause of mental deterioration in the elderly. Lancet 2 : 207-210, 1974
7) 東海林幹夫：アルツハイマー病の生物学的マーカーについて．第19回「大学と科学」公開シンポジウム講演収録集：アルツハイマー病；治療の可能性を探る・クバプロ，2005
8) 志賀裕正，武田 篤，荒井啓行，他：プリオン病診断のための臨床検査．第44回日本神経学会総会シンポジウム S3，横浜，2003.5
9) 日本老年医学会 編：高齢者の安全な薬物療法ガイドライン2005．東京，メジカルビュー社，2005
10) Okamura N, Suemoto T, Shimadzu H, et al : Styrylbenzoxazole derivatives for *in vivo* imaging of amyloid plaques in the brain. J Neurosci 24 : 2535-2541, 2004
11) Okamura N, Suemoto T, Shiomitsu T, et al : A novel imaging probe for *in vivo* detection of neuritic and diffuse amyloid plaques in the brain. J Mol Neurosci 24 : 247-255, 2004